Emittance Preservation in a possible ILC Main Linac which follows the Earth's Curvature

Nick Walker[1]

September 05, 2005

Abstract

I present here some preliminary studies of the application of Dispersion Free Steering (DFS) to a possible 250-500 GeV ILC main linac which follows the Earth's curvature (assuming a constant radius). For a direct comparison, results for the same linac with a laser-straight geometry are also presented.

[1] DESY, Hamburg, Germany

1. Introduction

It is well known that application of beam-based alignment is mandatory for the ILC main linac in order preserve (to within some budget) the tiny vertical emittance required for high luminosity. Over the last decade, many studies have been made of various emittance tuning algorithms (beam-based alignment) with varying degrees of sophistication for the model used (see for example [1-3]). However, to date, all such simulations have assumed a laser-straight geometry for the main linac. Such a configuration – while conceptually appealing from the point of view of beam dynamics – has both cost and engineering implications. In the TESLA TDR [4], the main linac followed the Earth's curvature in a shallow tunnel with an average depth of ~20m. The choice of tunnel layout was driven by civil engineering costs, and issues with the cryogenics. While rough estimates were made on the impact of this curved geometry on the beam dynamics, the implications for the beam-based alignment algorithms were never considered in detail or simulated.

The TESLA TDR solution assumed a smooth following of the Earth's curvature, with the required vertical bending being supplied by the FODO lattice and the dipole corrector windings on each quadrupole. No additional vertical bends where foreseen. This solution is probably the cheapest possible, and represents one extreme of the spectrum of possibilities, the other extreme being the laser-straight approach. There are naturally half-way solutions using two or more laser-straight segments separated by the required vertical bending sections.

In this report, I will investigate the impact of the TESLA TDR layout as one possible option for the ILC. We will focus on the use of a so-called Dispersion Free Steering algorithm (DFS), since such methods has been extensively studied in the past. We should note that the object of this study is to ascertain if there is any significant degradation in performance between a laser-straight geometry and one that follows the Earth's curvature, and is not intended as a comprehensive study of DFS algorithms or their performance. With that in mind, an idealised and simplified DFS algorithm has been used to compare the two configurations. I have included a brief overview of the approximations used, and a discussion of their possible impact to the results. A detailed explanation of the simulation is given in Append A.

2. Linac configuration and errors simulated

2.1 Basic linac parameters

In the absence of any detailed linac lattice for the ILC, I have chosen to study a simple 500 GeV machine (for the 1 TeV centre-of-mass upgrade) consisting of a contiguous linac with a constant β lattice. I have essentially taken the TESLA high-energy linac configuration which uses six 12-cavity cryomodules per 60° fodo cell. I have chosen 35 MV/m as the active gradient. Details of the linac configuration are given in Table 1.

Table 1: Basic linac parameters used for the simulations.

Gradient	35	MV/m
RF phase[2]	4.4	°
# cavities / cryomodule	12	
cryomodule / cell	6	
β_{max}	172	m
$\Delta\phi_{cell}$	60	°
L_{cell}	99.5	m
Int. quadrupole strength	0.02	m^{-1}
$E_{initial}$	5	GeV
E_{final}	505	GeV
initial RMS $\Delta p/p$	2.8	%
# quadrupoles	385	
# cryomodules	1153	
# cavities	13836	

2.2 Earth curvature configuration

To follow the average curvature of the Earth (assuming $r_{earth} \approx 6000$ km), a small vertical angle of 2.72 µrad was applied at the exit of each cryomodule as depicted in figure 1. It is assumed that the curvature is compensated for by steering the beam using the vertical corrector dipoles. (Steering the ~3 µrad per cryomodule corresponds to an effective quadrupole offset of ~450 µm.) Figure 2 shows a section of the design beam trajectory through a section of the linac (relative to the curved geometry). The resulting systematic offset of (maximum) 50 µm through the intervening cavities is small compared to the expected 500 µm RMS cavity alignments foreseen.

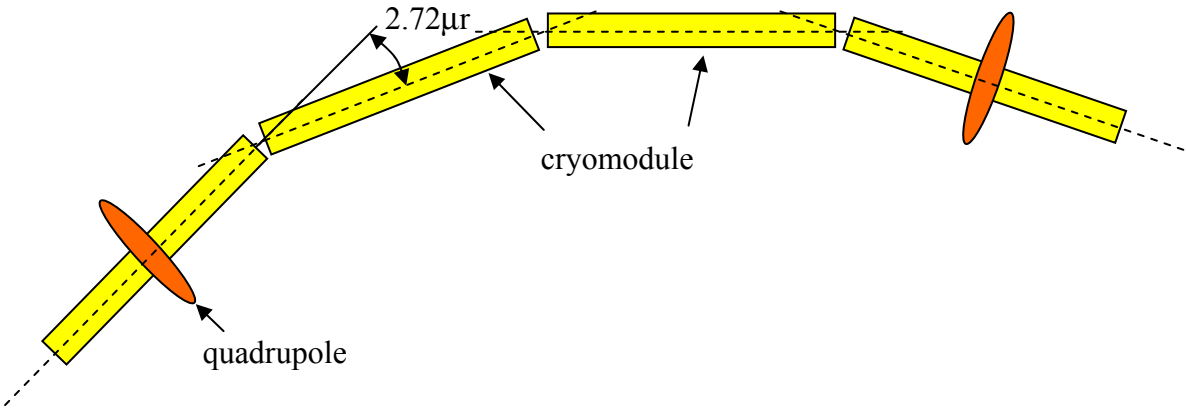

Figure 1: Sketch of Earth curvature following linac geometry

While the radius of curvature is very small, the resulting vertical dispersion is not negligible, and must be matched to prevent excessive emittance dilution due to filamentation. The 'matched' maximum vertical dispersion is approximately 1.1 mm (see section 5).

[2] Minimum RMS energy spread for a 300 µm bunch with 2×10^{10} particles. No BNS damping assumed.

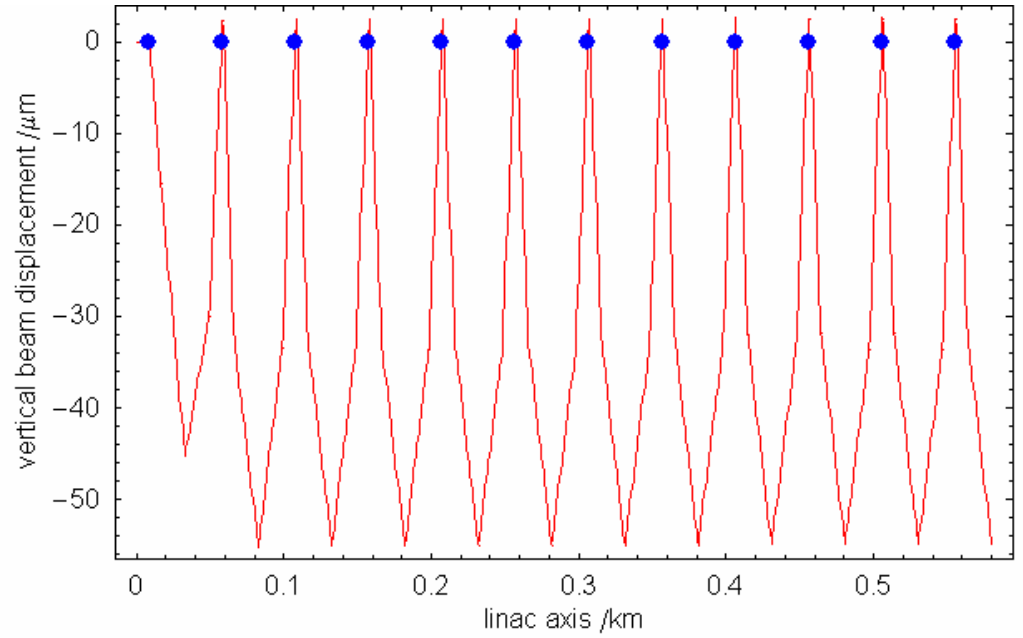

Figure 2: Design orbit relative to the curved geometry of a section of linac which follows the Earth's curvature. The blue dots correspond to the BPM locations (zero by default after steering).

2.3 Modelled alignment errors

Table 2 gives the RMS values used for the random component alignment errors.

Table 2: RMS component errors used in the simulations.

component	ref. axis	type	RMS	
Cavity	cryomodule	offset	300	μm
		tilt	300	μrad
Quadrupole	cryomodule	offset	300	μm
		roll	300	μrad
BPM	cryomodule	offset	200	μm
BPM noise	BPM		5	μm
Cryomodule	accel. reference	offset	200	μm

3. Dispersion Free Steering (DFS) reviewed

As the name implies, DFS attempts to find an orbit (trajectory) which is 'dispersion free'. Most DFS algorithms attempt to minimise the measured difference orbit generated by a finite change in energy of the beam. If $\mathbf{y}(\delta)$ is a vector of the 'measured' trajectory for a given momentum error $\delta = \Delta p/p_0$, then we can write

$$\Delta\mathbf{y}(\delta) = \mathbf{y}(\delta) - \mathbf{y}(0) = \mathbf{Q}(\delta)\cdot\boldsymbol{\Theta} \qquad (1)$$

where $\boldsymbol{\Theta}$ is a vector of dipole correction settings, and $\mathbf{Q}(\delta)$ is the linear chromatic response matrix of the lattice. The elements of $\mathbf{Q}(\delta)$ are given by

$$Q_{ij}(\delta) = \begin{cases} g_{ij}(\delta) - g_{ij}(0) & i > j \\ 0 & i \le j \end{cases} \tag{2}$$

where the $g_{ij}(\delta)$ are the linear Greens functions from the j^{th} corrector to the i^{th} measurement location (BPM).

Conceptually, the approach is to find a corrector solution which results in the measured orbit difference, and then subtract that solution from the current corrector settings, i.e.

$$\mathbf{\Delta\Theta} = -\mathbf{Q}^{-1} \cdot \mathbf{\Delta y} \tag{3}$$

The result is a 'dispersion free' trajectory (at least at the BPMs). In practise, the presence of small measurement errors causes the resulting absolute trajectory for exact solutions of equation (3) to have unphysically large deviations from the nominal reference axis. To avoid this behaviour, the approach generally taken is to soft-constrain the absolute trajectory ($\mathbf{y}(0)$) to within the expected alignment errors of the monitors. The problem now becomes over-constrained and must be solved in a least squares sense by minimising

$$\chi^2 = \frac{\mathbf{\Delta y}(\delta) \cdot \mathbf{\Delta y}(\delta)}{\sigma_{res}^2} + \frac{\mathbf{y}(0) \cdot \mathbf{y}(0)}{\sigma_{BPM}^2} \tag{4}$$

The weights σ_{res} and σ_{BPM} are generally taken as the BPM resolution (noise) and the expected RMS BPM offset respectively. The resulting dispersion ($\mathbf{\Delta y}$) is no longer exactly zero, but with a correct choice of weights can be made acceptably small, while at the same time a realistic absolute trajectory is maintained.

3.1 Generalised Dispersion Steering

Having introduced the usual more specialised case of dispersion *free* steering, it is relatively simply to extend the algorithm to include a non-zero *design* dispersion, as required for an Earth curvature following geometry. In the more general case, $\mathbf{\Delta y}(\delta)$ is given by

$$\mathbf{\Delta y}(\delta) = \mathbf{y}(\delta) - \mathbf{y}(0) - \mathbf{\Delta y}_{nom}(\delta), \tag{5}$$

where $\mathbf{\Delta y}_{nom}(\delta)$ is the nominal or design difference orbit for the momentum error δ. The corrector solution is found as before by minimising equation (4). An example of a segment $\mathbf{\Delta y}_{norm}(\delta)$ is shown in figure 3.

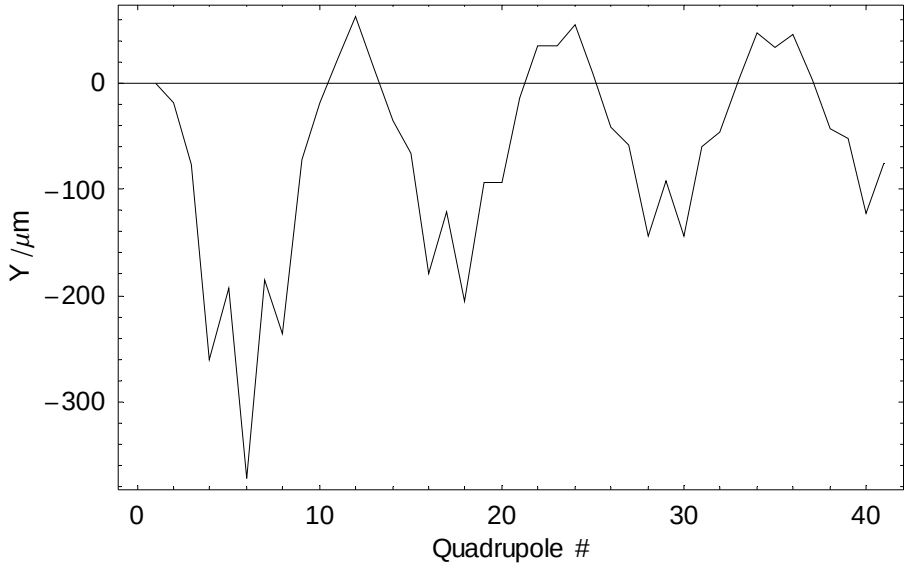

Figure 3: Example of the design dispersive orbit (first segment of 40 quadrupoles), for an initial energy change of -20% (only BPM locations shown)

4. Approximations used in the simulation

The results presented here have been produced using the simulation package Merlin [5]. Following the documented approach, the linac is divided up into overlapping segments, to which the DFS algorithm is applied in turn. In order to speed up the simulation (in particular the piecewise application of the DFS algorithm) several approximations have been made:

- For the DFS trajectory correction, a single ray was tracked representing the beam centroid. This ignores the effects of wakefields and beam filamentation which could perturb the beam centroid. However, for the ILC these effects are generally small, and can in principle be mitigated by iterating the procedure. The results reported below are obtain using a 'single-shot' correction (i.e. no further iteration was applied).
- Full simulation of the energy adjustment was not made; instead the initial energy of the centroid modelling ray was simply adjusted by the required amount. Changing the initial momentum is usually performed by adjusting the acceleration of the upstream linac sections, which generally perturbs the beam trajectory due to the cavity tilts. It is important to either control the launch condition into the section with feedback, or to use the first few BPMs to fit the incoming difference out. This important effect has been effectively ignored for this study.
- Beam jitter was not modelled, and no correction for the initial beam trajectory was made.

Once the DFS algorithm has been applied, a single bunch represented by longitudinally sliced macro-particles is tracked (including wakefield effects) in order to determine the final beam emittance.

Given that this study represents a first investigation of the potential impact of following the Earth's curvature, I consider the above approximations to be justified, even though they ignore effects which are know to impact the performance of DFS algorithms. Full detailed simulations still need to be done.

5. The design machine

As a first step, we check the emittance performance of the design machine which follows the Earth's curvature as described above. The linac model (including the vertical angles) was first constructed, and the dipole correctors at each quadrupole were adjusted to give zero offset at the BPMs (note for the design machine, there are no offset errors). This 'design' model was then used for all subsequent estimates of response matrices and nominal dispersive trajectories.

The resulting normalised vertical emittance is shown in figure 4. The matched dispersion condition at the beginning of the linac was artificially introduced into the initial beam (i.e. no matching section was constructed). Since there is approximately 1 mm of vertical dispersion by design, this contribution must be removed in order to see the residual emittance growth. The emittance plotted in Figure 2 is calculated by removing the linear momentum correlation from the second-order moments of the beam before calculating the emittance. An emittance growth of ~0.1 nm is observed, corresponding to 0.5% which can be considered negligible.

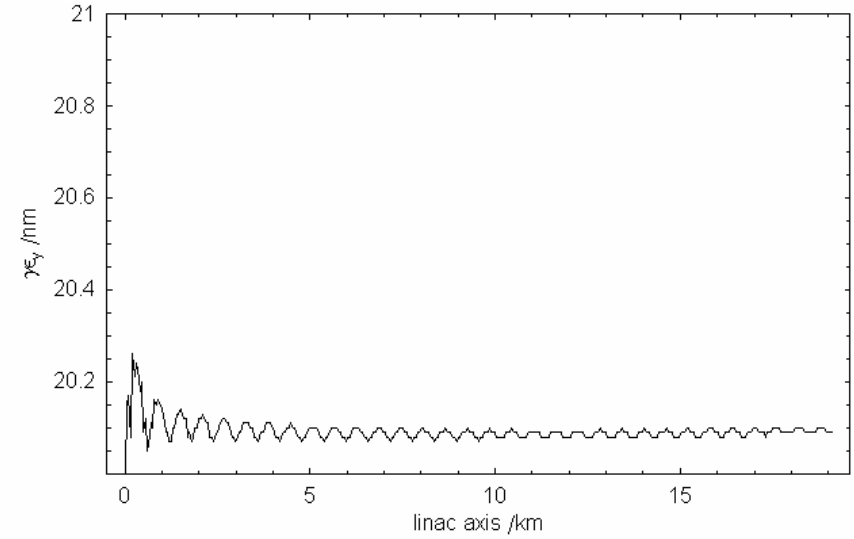

Figure 4: Design emittance for a perfect linac following the Earth's curvature.
Note that the effect of the momentum correlations have been removed. The initial emittance is 20 nm.

Inclusion of the design vertical dispersion increases the projected emittance as follows:

$$\gamma\Delta\varepsilon \approx \gamma\frac{\left(\hat{\eta}_y\delta_{RMS}\right)^2}{\hat{\beta}_y} = \begin{cases} 54\,\text{nm} & E_{beam} = 5\,\text{GeV} \\ 0.54\,\text{nm} & E_{beam} = 500\,\text{GeV} \end{cases} \tag{6}$$

6. Simulation results of DFS applied to random machines

In order to make a direct comparison between laser-straight and Earth curvature geometries, the same 1000 random set of alignment errors were used for both cases. In the case of the Earth curvature geometry, the initial beam contained the matched dispersion correlation. In both cases, the resulting emittance was calculated by first removing the linear momentum correlation as described above. By removing the momentum correlations from the laser-straight results – where there is no *design* dispersion – we are able to make a fair comparison between these and the Earth curvature results. We should note in passing that there is also an

expected gain (reduction) in emittance growth by removing the correlation for the laser-straight results, since the residual dispersive emittance growth does not completely filament.

The algorithm simulated applied DFS to linac sections containing 40 quadrupoles, overlapping by 20 quadrupoles. Two models for the momentum change were studied:

- A fixed momentum change of −1 GeV, (−20% of the initial 5 GeV beam energy) was applied at the start of each segment. In this case the relative momentum change scales inversely with energy along the linac (−20% at 5 GeV, to −0.2% at 500 GeV).
- A fixed relative momentum change of −20% was applied at the start of each segment (−1 GeV at 5 GeV, to −100 GeV at 500 GeV).

Figures 5 and 6 shows the simulation results 1000 random 250 GeV linacs and 500 GeV linacs respectively. Tables 3 and 4 summarises the fractions of seeds achieving less than or equal to 30 nm, and the 90% emittance values.

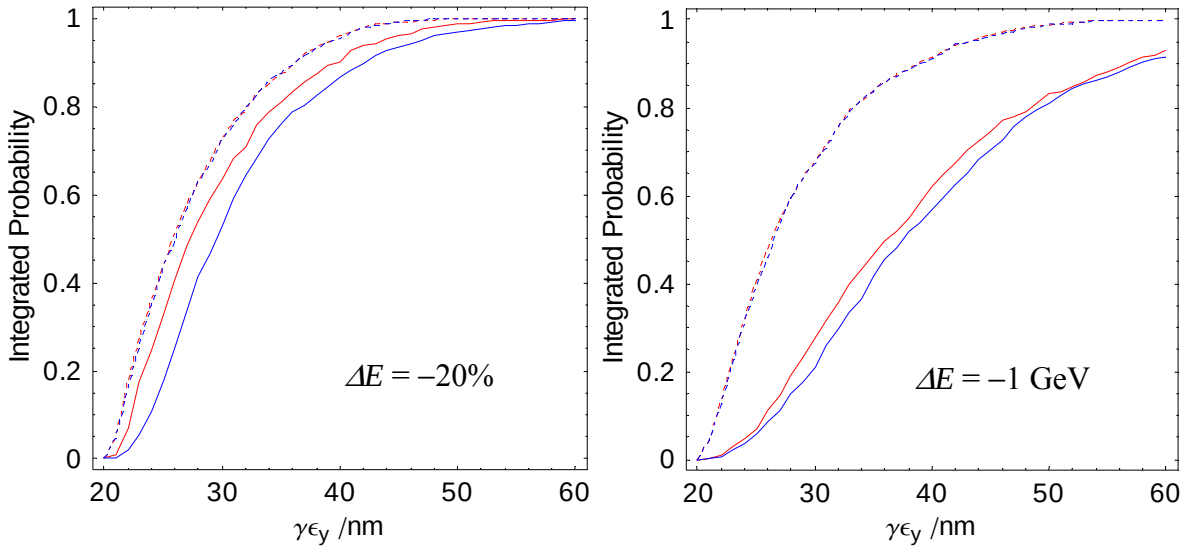

Figure 5: Simulations results of 1000 random 250 GeV linacs. The graphs indicate the fraction of the seeds resulting in less than or equal to the specified emittance. Red and blue lines show the results for the laser-straight and curved geometries respectively. Solid lines indicate the as calculate projected emittance, while the dashed lines show the emittance after removing the linear momentum correlation.

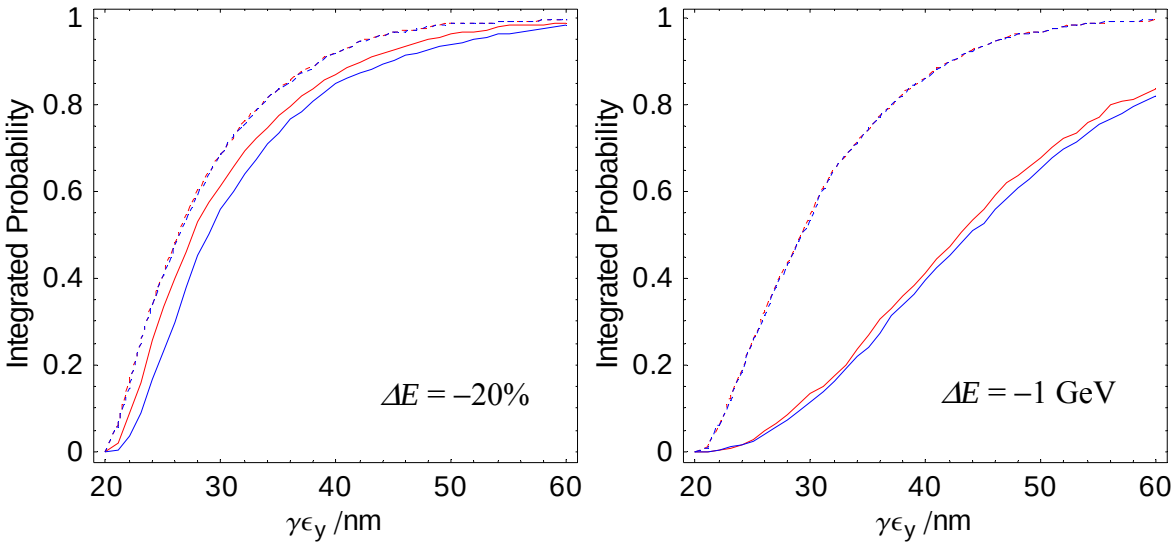

Figure 6: Simulations results of 1000 random 500 GeV linacs. See caption for figure 3 for details.

Table 3: Emittance summary results for 1000 random machines (linear momentum correlation removed). Note these sets of results are the same for both laser-straight and curved geometries.

ΔE_{DFS}	250 GeV		500 GeV	
	% ≤ 30 nm	90% limit	% ≤ 30 nm	90% limit
-20%	73%	36 nm	67%	39 nm
-1 GeV	68%	39 nm	54%	42 nm

Table 4: Projected emittance summary results for 1000 random machines.

	ΔE_{DFS}	Straight		Curved	
		% ≤ 30 nm	90% limit	% ≤ 30 nm	90% limit
250 GeV	-20%	64%	40 nm	53%	42 nm
	-1 GeV	28%	57 nm	21%	58 nm
500 GeV	-20%	61%	42 nm	56%	45 nm
	-1 GeV	13%	67 nm	12%	70 nm

7. Preliminary conclusions and further work

Within the constraints and approximations used for the simulations, it would appear that there is no significant impact on the achievable emittance from a linac which follows the Earth's curvature as compared to a laser-straight geometry, *providing* one takes into account the nominal vertical dispersion generated by the vertical bending; specifically:

- The vertical dispersion must in principle be matched at the entrance and exit of the linac to avoid emittance dilution due to filamentation. In principle empirical tuning of the dispersion at the entrance of the linac (using either a design matching section or simple dispersion generating orbit bumps) could be used to minimise the exit emittance (or maximise the luminosity). A similar dispersion correction at the exit of the linac would be beneficial for either geometry to remove the remaining non-filamented correlation, and the additional effect of the matched dispersion for the curved geometry is almost insignificant at the linac exit.

- During beam based alignment (dispersion steering), the design non-zero off-energy trajectory must be corrected to. This has implications for the BPM linearity and scale errors since we now expect to measure a non-zero difference orbit (worst case in these simulations was ~300 μm). A 10% BPM error over a 300 μm range would effectively result in approximately 30 μm/0.20 = 0.15 mm of residual (unmatched) dispersion, corresponding to $\gamma\Delta\varepsilon \approx 1\text{nm}$ at 5 GeV (worst case), which would appear negligible. (For the laser-straight geometry, DFS is effectively a nulling method, and the BPM non-linearity can in principle be mitigated by iteration, assuming that the method converges.)

The simulations reported here are simplistic given the assumptions and approximations outlined in section 4. For completeness it is important to increase the sophistication of the simulation to correspond to a more 'real world' model:

- A full beam representation should be tracked for the orbit measurements instead of the single ray approach used here; this would then include any wakefield or filamentation effects which could perturb the orbit during the off-energy measurements. As with the BPM linearity, the systematic impact of wakefields on the non-zero off-energy design trajectory needs to be evaluated. The wakefield-induced perturbation of the off-energy orbit could again lead to an additional unmatched residual dispersion (although at least in principle this could be modelled). This effect is expected to be small (see Appendix B).
- The energy change should be realistically generated by adjusting the linac RF. The primary difference here will be the effect of RF steering due to the expected cavity tilts, which will modify the launch condition into the correction segment. Most implementations of DFS deal with this by either assuming the launch conditions are maintained by re-steering (feedback), or that the launch condition is fitted out from the resulting measured BPM data. In both cases the resolution of the chosen BPMs at the segment boundaries play an important role, and generally degrades the performance of the correction; this situation should however be identical for both laser-straight and curved geometries.
- Pulse to pulse random jitter needs to be included in the simulations. Purely random jitter (white noise) can in principle be average away, however at a few Hz rate this may be costly in time, and may be compounded by the dangers of slower systematic drifts. The preferred method is to take single-shot measurements and again use the first few BPMs to determine the launch condition and remove it from the measured data, as for the RF steering described above. In this case the same comments concerning BPM resolution apply.

The final comments concern the DFS algorithm itself and understanding its limitations. The impact of systematic errors (knowing the energy for example), quadrupole errors, modelling errors etc. all have the potential to significantly degrade the performance. These are outstanding issues for study irrespective of the chosen geometry, and are quite likely to have a larger impact on the ultimate performance of DFS than the choice of geometry.

Appendix A: Details of the Merlin simulation

The reported simulations were made using the Merlin package. The algorithm applied used the following steps (per random seed):

1. Two models of the linac were constructed, both containing the 2.72 μr vertical kinks at the exit of the cryomodules as discussed above. The first model – the *reference* model – was steered to exactly zero the BPM readings (no errors); this model represents the design machine and is used for all subsequent calculations of design orbits, response matrices etc. The second model – the *simulation* model – has a complete set of random alignment errors applied to it, and is used to simulate a quasi-realistic machine.
2. Beam-based alignment is applied to the simulation model in segments of 40 quadrupoles with an overlap of 20 quadrupoles. Hence the first alignment segment is from quadrupoles 1-40, the second from 20-60 etc.
3. Two rays are first constructed, $\mathbf{x}_{ref}$ and $\mathbf{x}_{sim}$, representing the bunch centroid for the reference and simulation model respectively. They are both initially set to zero.
4. For each alignment segment:
    a. $\mathbf{x}_{ref}$ is tracked thought the corresponding segment of the reference model both on energy and with the required energy deviation. The resulting BPM difference orbit is used as the design difference trajectory.
    b. The response matrix is constructed using the reference model by tracking a single ray, and systematically adjusting each corrector in the segment by a small amount, and recording the subsequent response of the BPMs. This is done for both nominal and off-energy, and the two resulting matrices subtracted to give the required matrix for DFS.
    c. $\mathbf{x}_{sim}$ is tracked through the corresponding segment of the simulation model on and off energy, and the BPM readings (including noise) are recorded. The difference trajectory is then calculated.
    d. A correction (equations 4 and 5) for the difference trajectory from the simulation model is calculated using SVD. The on-energy trajectory from the simulation model is used as the absolute soft constraint. The weights used were $1/(\sqrt{2}\times 5\mu\text{m})$ and $1/(360\mu\text{m})$ for the difference and absolute BPM measurements respectively.
    e. The calculated correction is applied to the correctors in the segment of the simulation model.
    f. $\mathbf{x}_{ref}$ and $\mathbf{x}_{sim}$ are tracked (updated) through the reference and simulation models to the starting point of the next segment.
    g. Steps *a-f* are repeated for the next segment.
5. One the entire linac has been beam-based aligned in the above fashion, a single-bunch represented by sliced macro-particles is tracked (including wakefields) to estimate the final resulting emittance dilution. The bunch represents $\pm 3\sigma_z$ longitudinal extent, divide into 31 slices. Each slice contains 11 macro-particles representing the initial uncorrelated energy spread. The correct $\langle y\delta \rangle$ and $\langle y'\delta \rangle$ correlation representing the matched dispersion is introduced into the bunch before tracking.

Appendix B: Impact of Wakefields

Figure 7 shows the results of a $\Delta E / E = -20\%$ trajectory for the first 40 quadrupoles. The red solid line shows the result for single-particle tracking, while the blue dashed line shows the result of a full bunch simulation, including wakefields. The magenta dashed line indicates the difference of the two results (multiplied by 10).

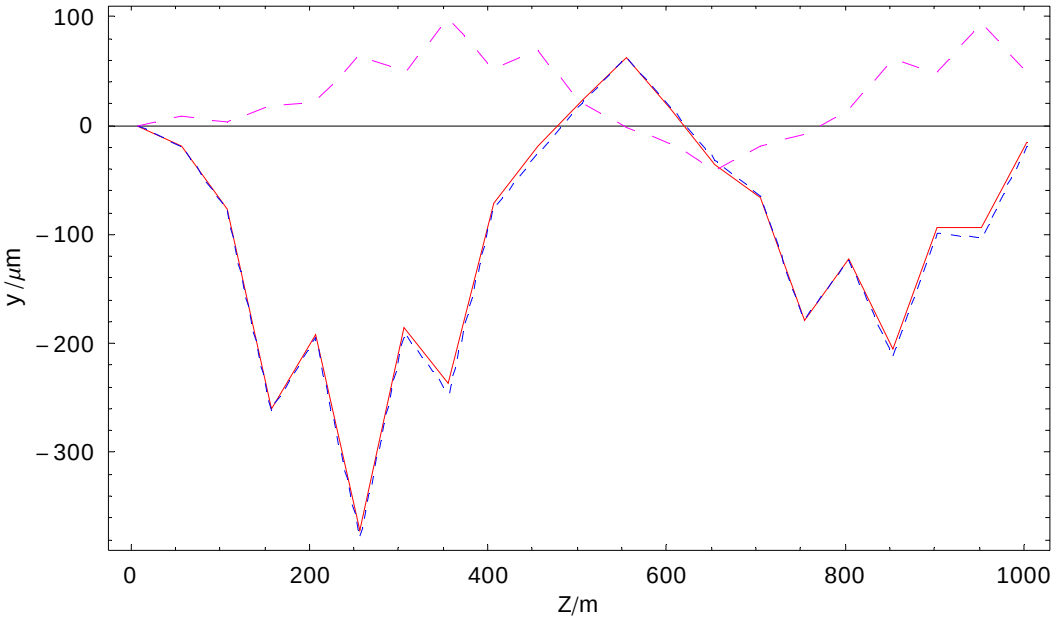

Figure 7: Effect of wakefield on off-energy trajectory for the first 40 quadrupoles. The red solid line is the result of tracking a single particle representing the bunch centroid (no wakefields), as used in the reported simulations; the blue dashed line is the simulation of the full bunch including wakefields; and the magenta dashed line is the difference (×10).

The error of not including wakefield effects during the simulation of the measurement would appear to be of the order of 10 μm peek, resulting in a systematic residual dispersion of 10 μm/0.2 = 50 μm. Again taking $\hat{\beta}_y = 172\text{m}$, we have $\gamma\Delta\varepsilon_y \approx 0.1\text{nm}$ (E_{beam} = 5 GeV) which is negligible.

Acknowledgement

This work is supported by the Commission of the European Communities under the 6th Framework Programme "Structuring the European Research Area", contract number RIDS-011899.

References

1 BRIEF REVIEW OF LINEAR COLLIDER BEAM BASED ALIGNMENT FOR LINACS.
By Tor Raubenheimer, Peter Tenenbaum (SLAC),. SLAC-TN-03-071, LCC-0129, Mar 2004. 7pp.

2 BEAM BASED ALIGNMENT OF THE TESLA MAIN LINAC.
By P. Tenenbaum (SLAC), R. Brinkmann (DESY), V. Tsakanov (Yerevan Phys. Inst.),. SLAC-PUB-9264, Jun 2002. 4pp. Presented at 8th European Particle Accelerator Conference (EPAC 2002), Paris, France, 3-7 Jun 2002. Published in *Paris 2002, EPAC 02* 515-517

3 SIMULATIONS OF THE STATIC TUNING FOR THE TESLA LINEAR COLLIDER.
By D. Schulte (CERN), N. Walker (DESY),. DESY-M-03-01Q, Jun 2003. 3pp.
Prepared for Particle Accelerator Conference (PAC 03), Portland, Oregon, 12-16 May 2003.

4 TESLA TECHNICAL DESIGN REPORT PART II, By R. Brinkmann, (ed.), K. Flottmann, (ed.), J. Rossbach, (ed.), P. Schmuser, (ed.), N. Walker, (ed.), H. Weise, (ed.) (DESY & Hamburg U.),. DESY-01-011, DESY-2001-011, DESY-01-011B, DESY-2001-011B, DESY-TESLA-2001-23, DESY-TESLA-FEL-2001-05, ECFA-2001-209, Mar 2001.

5. http://www.desy.de/~merlin